

(NASA-TM-78592) A NEW BASIS FOR THE  
DETERMINATION OF FRACTURE TOUGHNESS (NASA)  
49 p HC A03/PF A01 CSCL 20K

N79-23256

Unclas  
G3/31 20834

---

# A New Basis for the Determination of Fracture Toughness

---

S. Banerjee

---

May 1979

**NASA**  
National Aeronautics and  
Space Administration



---

# **A New Basis for the Determination of Fracture Toughness**

---

**S. Banerjee, Ames Research Center, Moffett Field, California**



National Aeronautics and  
Space Administration

**Ames Research Center**  
Moffett Field, California 94035

## NOMENCLATURE

$a$	Crack length
$B$	Thickness
$E$	Young's modulus
$E'$	A measure of strain hardening in the assumed bilinear stress-strain behavior of the material vide equation (1)
$f$	Compliance function, $E\nu B/P$
$F$	K calibration factor, $K/PB\sqrt{W}$
$K$	Stress intensity factor
$K_{IC}$	Value of stress intensity at which the crack starts growth
$[K_{IC}]_{399}$	ASTM E399 valid plane strain fracture toughness
$K_f(\max)$	is the maximum value of stress intensity used during the final stages of fatigue cracking
$K_R$	Plasticity corrected stress intensity factor value corresponding to a given crack extension as in the R-curve determination
$K_Q$	Stress intensity factor corresponding to 2% crack extension as measured by the secant technique
$K^*$	Stress intensity factor corrected for plasticity as per equation (4)
$m$	Yielding constraint in K-R relationship in equation (2b)
$M$	Yielding constraint in $K-R_{eff}$ relationship in equation (2a)
$P$	Load
$r$	Distance from the crack tip along $x$ direction
$R$	Plastic zone size
$R_{eff}$	Nominal plastic zone size
$W$	Width
$W_c$	Critical width at which the crack initiates

$\sigma_{yy}$	Normal stress in y direction
$\sigma_Y$	Uniaxial yield strength determined according to .02 offset procedure
$\epsilon_{yy}$	Normal strain in y direction
$\epsilon_Y$	Yield strain and is equal to $\sigma_Y/E$
$V$	Total displacement
$V_e$	Elastic component of the displacement
$\Delta V$	Total deviation from the linear displacement
$\Delta V_p$	Deviation from linear displacement due to the growth of plastic zone
$\Delta V_c$	Deviation from linear displacement due to the growth of crack
$\Delta a$	Total crack extension
$\Delta a_c$	Physical crack extension
$\Delta a_p$	Crack extension equivalent to the growth of plastic zone and is equal to $R_{eff}/2$

# A NEW BASIS FOR THE DETERMINATION OF FRACTURE TOUGHNESS

S. Banerjee\*

Ames Research Center

## INTRODUCTION

Plane strain fracture toughness,  $K_{IC}$ , is a property of a material and is expected to be independent of the size, configuration, and loading of the specimen or the structure. A procedure for the determination of  $K_{IC}$  is described in ASTM E399 [1].<sup>1</sup> In this procedure, the start of crack growth is identified by the deviation from linearity in the load-displacement test record. This approach is simple and reasonable. But plasticity preceding or accompanying the crack growth is not considered in a satisfactory manner which can cause  $K_Q$  or, in some cases,  $K_{IC}$  to depend on the specimen width.

A new approach is proposed here which gives a width-independent  $K_{IC}$  value. In the new approach,  $K_{IC}$  is defined as the value of the stress intensity factor,  $K$ , at which the crack starts physical extension. The approach is based on the results of approximate analyses and supporting experimental data. At first, the existing approaches to the determination of  $K_{IC}$  are examined. Then, an analysis is presented which demonstrates that the growth of the plastic zone and the constraint in a compact tension specimen can depend significantly on the specimen width. Afterward, a typical R-curve [2] is analyzed to evaluate the simultaneous contribution of crack growth and crack tip plasticity to the observed deviation from

---

\*Senior NRC Resident Research Association on leave from the India Institute of Technology, Bombay.

<sup>1</sup>The italic numbers in brackets refer to the list of references appended to this paper.

linear elastic behavior. A combination of these two analyses produces a very simple procedure for the determination of fracture toughness. The final discussion includes a comparison of the analytically predicted and experimental results, a description of the proposed approach, and the implications of the results obtained.

#### EXISTING APPROACHES TO THE DETERMINATION OF $K_{IC}$

In ASTM E399 [1], the load,  $P_Q$ , corresponding to the start of crack growth is identified by the 5% secant technique. The 5% secant is supposed to correspond to an equivalent crack extension of 2%.

According to ASTM E399, three possible types of load-displacement test records are obtained during the testing of the precracked specimens. A material with low toughness and high yield strength in which the crack extension occurs abruptly gives what is termed a Type-III load-displacement test record [1]. The value of  $K_{IC}$  calculated from  $P_Q$  in such a case is largely independent of the size of the specimen. The Type-II load-displacement test record is similar to the Type III in this respect. However, in materials with somewhat higher toughness, the crack and plastic zone grow simultaneously. This type of behavior gives a Type-I load-displacement test record. According to E399, in such a case, the value of  $K_Q$  computed from  $P_Q$  is considered to be a valid  $K_{IC}$  measurement if the following two conditions are satisfied: (a) the specimen thickness,  $B \geq 2.5 (K_Q/\sigma_Y)^2$  where  $\sigma_Y$  is the yield strength; and (b)  $P_{max}/P_Q \leq 1.1$  where  $P_{max}$  is the maximum load encountered during the loading of a precracked body. For clarity, the  $K_{IC}$  obtained in such a manner will be

referred to as  $[K_{IC}]_{399}$ . Recent experiments [3-9] have shown that  $K_Q$  and, in some instances, the valid  $[K_{IC}]_{399}$  depend on specimen width  $W$ .

ASTM E399 implicitly assumes that the plastic zone size depends only on specimen thickness and is independent of width. On the other hand, the width dependence of  $K_Q$  or  $[K_{IC}]_{399}$  values is observed in the compact tension specimens which satisfies the ASTM E399 requirement that the thickness  $\geq 2.5 (K_Q/\sigma_Y)^2$ . Further, the experimental data indicate that the thickness has only a small effect on  $K_Q$  values obtained from the compact tension and three-point bend specimens. It thus appears that a large thickness cannot guarantee a limited plasticity during the start of crack growth unless the width is correspondingly increased.

The second condition above, concerning  $P_{max}/P_Q$ , is specified to guarantee that the deviation from linearity is produced primarily by crack extension. The condition that  $P_{max}/P_Q \leq 1.1$ , can be achieved only when the R-curve [2] is flat; where the R-curve is a plot of stress intensity factor corrected for plasticity versus the corresponding physical crack extension. For a given material, a load-displacement test record which satisfies the requirement that  $P_{max}/P_Q \leq 1.1$ , can be obtained in a very limited combination of specimen size and configuration. A specimen is tested in a laboratory to simulate the behavior of a structure in service. Yet the form of load-displacement test record of the specimen where  $P_{max}/P_Q \leq 1.1$  may not correspond to the form observed in a real engineering structure. Therefore,  $[K_{IC}]_{399}$  of a material measured in a specimen where  $P_{max}/P_Q \leq 1.1$  may not be meaningful in predicting the fracture behavior of a structure where  $P_{max}/P_Q > 1.1$ .

The problem of the width dependence of  $K_Q$  values has been examined by others. Kaufman [5] has proposed a relaxation of the  $P_{max}/P_Q$  requirement and the use of specimens with thickness/width ratios of less than 0.5. Newman [10] has suggested a two-parameter approach to predict toughness in specimens with varying widths. This approach is empirical and is concerned with the maximum load at failure and therefore relates to the final propagation rather than the start of the crack growth. Munz [3] has proposed an approach where the toughness is based on the actual point of crack extension. He has recommended a variable secant technique where the secant value is adjusted according to specimen width.

#### PLASTICITY, CONSTRAINT, AND WIDTH OF A COMPACT TENSION SPECIMEN

Recently, it has been shown through a simple and approximate analysis [11-13] that the width and crack length of single-edge notch specimens at a given value of  $K$  significantly influence the nominal plastic zone size, the yielding constraint, and the crack opening displacement (COD). These results are in qualitative agreement with the recently reported experimental observation that the value of  $K_Q$  increases with increasing width [3-9]. The width dependence of  $K_Q$  suggests that the growth of the plastic zone ahead of the crack tip may be dependent on the specimen width. On the other hand, the two-dimensional finite element analyses do not give entirely satisfactory results. For instance, the plastic zone size can be considered equivalent to a virtual crack extension. Accordingly, the displacement of the specimen depends on the plastic zone size. But the finite element analyses give width-dependent



plasticity-induced displacement values that are substantially less than the experimentally determined ones [3] particularly when the plastic zones are small. Thus, the reported two-dimensional analyses do not give a satisfactory representation of the growth of small plastic zones. In fact, it must be recognized that the crack tip deformation in the fracture toughness specimen is a three-dimensional elastic-plastic boundary value problem. Since such a problem is not satisfactorily resolved as yet, the simple and approximate analysis reported earlier [11-13] is used to evaluate the effect of specimen width on the displacement, constraint and the  $K_Q$  value. What follows in this section is a brief outline of this analysis and a comparison of the experimental and the analytical results. The good agreement between the experimental and the analytical results validate the analysis reported here.

The loading of a compact tension specimen can be satisfactorily represented by the combination of an axial force applied at the midpoint of the ligament ( $W-a$ ) and a bending moment [14]. An  $(r)^{-1/2}$ -type strain distribution at distances close to the crack tip is assumed, where  $r$  is the distance from the crack tip. The assumption follows from experimental observations [15-17]. The linear  $(-r)$  type distribution arises because of the bending of the compact tension specimen [18]. Experimental observations confirm that such a composite strain distribution exists ahead of the crack [19]. The composite strain distribution is schematically presented in Fig. 1. a plot of local strain  $\epsilon_{yy}$  against the distance  $X$ , measured from the tip of a crack of length  $a$ . The strain,  $\epsilon_{yy}$ , is related to the stress,  $\sigma_{yy}$ , through an assumed bilinear stress-strain behavior of the material which can be represented by

$$\left. \begin{aligned} &\sigma_{yy} = \epsilon_{yy} E \quad \text{for} \quad \epsilon_{yy} < \epsilon_Y \\ \text{and} \quad &\sigma_{yy} = \epsilon_Y E + (\epsilon_{yy} - \epsilon_Y)E' = \sigma_Y + (\epsilon_{yy} - \epsilon_Y)E' \quad \text{for} \quad \epsilon_{yy} \geq \epsilon_Y \end{aligned} \right\} (1)$$

where  $E'$  is a measure of the strain hardening of the material. In the subsequent results calculated and reported here,  $E'$  is assumed to be equal to  $E/150$ . It may, however, be noted that the results correspond to a limited amount of crack tip yielding, and therefore are not significantly influenced even if  $E'$  is assumed to have a value 3 times less, that is  $E/450$ .

As mentioned above, the analytical results reported here correspond to a limited amount of crack tip plasticity. Therefore, the plastic zone and the strains at the crack tip are rather small. Thus, the conversion of the strain into stress through equation (1) is a reasonable procedure. The bending moment and the axial force can then be written in terms of the  $\sigma_{yy}$  stress.

Based on the composite strain distribution (Fig. 1), load and moment balance equations were formulated. These equations were solved using Brown's method [20]. From this, the strain reversal point,  $X_2$ , and the plastic zone size,  $R = (X_2 - X_1)$ , were obtained. The loadline and crack mouth opening displacements of a compact tension specimen computed according to the above procedure agree well with the experimentally observed values [12].

The load-moment balance equations were solved for progressively increasing loads for a given specimen size. The calculations were performed

for different widths at  $a/w = 0.4, 0.5$ , and  $0.6$  to evaluate the effect of width and crack length on the value of  $R$  at different loads.

As shown in Fig. 1, the nominal plastic zone size,  $R$ , is defined by the point ahead of the crack tip at which  $\epsilon_{yy} = \epsilon_Y$ , where  $\epsilon_Y$  is the yield strain and is equal to  $\sigma_Y/E$ . Therefore, at  $r = R$ ,  $\sigma_{yy} = \sigma_Y$ . Figure 2 is a plot of the strain,  $\epsilon_{yy}$ , versus  $r$ , the distance from the crack tip in the plane of the crack. When the load is small, the plastic zone size has the shape of a pair of horns as schematically presented in Fig. 2. The analytical results show that in such a situation the actual plastic zone size is approximately equal to  $R$ , the distance from the crack tip at which  $\epsilon_{yy} = \epsilon_Y$  [21]. Correspondingly, that is in the plane strain condition, the displacement and the change in compliance is produced by an effective plastic zone size,  $R_{eff}$ , which is less than  $R$  [22] as shown in Fig. 2. Both  $R$  and  $R_{eff}$  depend on the state of stress or the yielding constraint at the crack tip.

According to McClintock and Irwin [22],  $R_{eff}$  is related to  $K$  through a relationship

$$R_{eff} = (K/\sigma_Y)^2/M\pi \quad (2a)$$

where  $M$  is a measure of the yielding constraint. Likewise,  $R$  is related to  $K$  through a similar relationship

$$R = (K/\sigma_Y)^2/m\pi \quad (2b)$$

where  $m$  is also a measure of the yielding constraint. It is assumed in this paper that

$$R_{eff} = R/m \quad (3)$$

Substitution of Eqs. (2a) and (2b) in (3) gives  $M = m^2$ . Thus,  $m$  and  $M$  can be calculated if  $K$  and  $R$  are known.

The strain,  $\epsilon_{yy}$ , at a distance,  $r = r_{\text{eff}}$ , ahead of the crack tip can be obtained from Eq. (3) and the  $1/\sqrt{r}$  dependence of the strain  $\epsilon_{yy}$  as shown in Figs. 1 and 2. The  $1/\sqrt{r}$  dependence of the strain gives

$$\frac{(\epsilon_{yy})_{r=R_{\text{eff}}}}{(\epsilon_{yy})_{r=R}} = \left( \frac{R}{R_{\text{eff}}} \right)^{1/2} = (m)^{1/2}$$

Accordingly,

$$(\epsilon_{yy})_{r=R_{\text{eff}}} = \sqrt{m} (\epsilon_{yy})_{r=R} = \sqrt{m} \epsilon_Y$$

This result is shown schematically in Fig. 2.

The assumption of Eq. (3) is reasonable and is consistent with the following observation. At a stress intensity value corresponding to  $R_{\text{eff}}$  equivalent to 2% crack extension, the value of  $M$  calculated according to the analysis reported above is around 3. At higher stress intensities, the plastic zone size is large and the shape of the plastic zone tends to be circular. The state of stress in this case corresponds to the so-called plane stress case. Correspondingly,  $R_{\text{eff}} = R$  and  $M = m = 1$ . These observations are in general agreement with the proposed values of  $M$  for plain strain and plane stress conditions [22]. In addition, at  $r = R_{\text{eff}}$ ,  $\epsilon_{yy} = \sqrt{m} \epsilon_Y$  and correspondingly  $\sigma_{yy} \approx \sqrt{m} \sigma_Y$ . This result is consistent with the analytical results on elastic-plastic stress distribution and the nominal plastic zone size [21].

The results from our analysis are next examined through two different relationships:  $K^*/\sigma_Y \sqrt{W}$  as a function of  $\Delta V_p/V_e$  and  $K^*/\sigma_Y \sqrt{W}$  as a function

of  $\epsilon$ . The former is concerned with the growth of the plastic zone and the latter with the change in the yielding constraint.  $K^*$  is the stress intensity factor,  $K$ , corrected for plasticity according to equation (4) discussed presently.

#### $K^*/\sigma_Y\sqrt{W}$ and the Growth of the Plastic Zone

In the absence of crack growth, the growth of the plastic zone directly relates to the deviation from the linear elastic behavior. According to Irwin's concept of virtual crack extension [23], the effective crack length  $a_{eff}$  is given by

$$a_{eff} = a + R_{eff}/2 \quad (4)$$

where  $a$  is the physical crack length. The values of  $R_{eff}$  can be obtained from the solution of the load and the moment balance equation. The effective crack length  $a_{eff}$  is then obtained from equation (4) and is used to calculate  $K^*$  which is called the plasticity corrected  $K$  value. The stress intensity factor,  $K$ , is calculated from the physical crack length,  $a$ . It may be noted that the difference between  $K$  and  $K^*$  is rather small since the maximum value of  $R_{eff}$  that could be obtained from the analysis is small.

Values of  $R_{eff}$  can be used to calculate the deviation from linearity through the standard compliance relationship. The deviation from linearity is expressed in terms of  $\Delta V_p/V_e$ , where the terms  $V_e$  and  $\Delta V_p$  are the linear elastic displacement and the deviation from linearity produced by the growth of the plastic zone. The terms  $V$ ,  $\Delta V$ , and  $\Delta V_c$  are the total displacement, the total deviation from linearity and the deviation from linearity produced by the growth of the

crack, respectively. All these terms are schematically represented in Fig. 3.

An examination of the results obtained from the analysis outlined in Figs. 1 and 2 shows that the parameter  $K^*/\sigma_Y\sqrt{W}$  depends on the value of  $\Delta V_p/V_e$  as shown in Fig. 4.

The  $\Delta V_p/V$  value, for a plastic zone size equivalent to 2% crack extension, depends on  $a/W$ . This can be independently computed from the standard compliance relationship [24]:

$$(EB/P)V = f \quad (5)$$

where  $E$  is Young's modulus,  $B$  is thickness,  $P$  is load, and  $i$  is a function of  $a/W$  only. Differentiation of Eq. (5) gives

$$\frac{EB}{P} \Delta V_p = \frac{df}{da} \Delta a_p = \frac{df}{d(a/W)} \frac{\Delta a_p}{W} = f' \frac{\Delta a_p}{W} \quad (6)$$

where  $\Delta a_p$  is the virtual crack extension due to the growth of the plastic zone. As outlined in Eq. (4) and Fig. 3,  $\Delta a_p = R_{eff}/2$ . Divide Eq. (6) by (5) and obtain

$$\frac{\Delta V_p}{V_e} = \frac{f'}{f} \frac{\Delta a_p}{W} = \frac{f'}{f} \frac{\Delta a_p}{a} \frac{a}{W} \quad (7)$$

Table 1 lists  $\Delta V_p/V_e$  values for  $\Delta a_p/a = 0.02$  as calculated from Eq. (7) for the different  $a/W$  values. The corresponding values of  $K^*/\sigma_Y\sqrt{W}$  are obtained from Fig. 4 and are also reported in Table 1. As shown in the table, for  $R_{eff}$  equivalent to 2% crack extension, the corresponding value of  $K^*/\sigma_Y\sqrt{W}$  is approximately equal to 0.5 for the  $a/W$  ratios investigated. The  $K^*$  value obtained from  $K^*\sigma_Y\sqrt{W} = 0.5$ , corresponds to the value obtained by the secant technique of ASTM E399 and therefore  $K^* = K_Q$ . Thus, the analysis shows that  $K_Q^2/\sigma_Y^2W = 0.25$ . This result is later compared with the experimental  $K_Q$  values obtained for different widths.

### $K^*/\sigma_Y\sqrt{W}$ and the Yielding Constraint

The values of  $K^*$  and  $R$  obtained from the results of the analysis outlined in Figs. 1 and 2 can be used to determine values of  $m$  and  $M$  from Eqs. (1) and (2). As we have seen, both  $m$  and  $M$  are relative measures of the yielding constraint.

Variations in the parameter,  $K^*/\sigma_Y\sqrt{W}$ , with  $m$  for various values of  $a/W$  are shown in Fig. 5, which shows that as  $W$  is increased,  $m$  will increase. An increase in the value of  $m$  increases the crack tip local stresses and this, in turn, will cause a typical plane strain-type fracture. From Fig. 5 for  $a/W = 0.5$ ,  $m = 1.9$  at  $K/\sigma_Y\sqrt{W} = 0.5$ . The corresponding value of  $M$  will be about 3.6.

### Calculated and Experimental Values of the Parameter $K_Q/\sigma_Y\sqrt{W}$

It was shown that  $K_Q^2/\sigma_Y^2W = 0.25$  corresponds to a plastic zone size equivalent to 2% crack extension and signifies a value of the yielding constraint which is constant at a given  $a/W$ . Figure 6 compares the experimental and the calculated relationship,  $(K_Q/\sigma_Y)^2$ , versus  $W$  for a variety of materials: low-strength steels [3]<sup>2</sup> and aluminum alloys [3,6]. The  $K_Q$  values reported are obtained under conditions where crack growth is absent. The scatter of the data in the figure may be caused by the usual errors in the determination of  $K_Q$ .

Errors in the experimentally determined  $K_Q$  value can arise due to the following reasons: (a) the friction at the loading pins and at the supports for the clip gauge affects the load-displacement test record;

---

<sup>2</sup>S. Banerjee, unpublished work.

(b) the secant value used to determine  $K_Q$  depends on  $a/W$  and should be calculated from Eq. (7). Instead, quite often, a 5% secant as recommended in ASTM E399, is used for all  $a/W$  ratios; (c) inadequate accuracy of the load-displacement test record introduces error in the secant measurements; and (d) the maximum stress intensity value used for fatigue cracking,  $K_f(\max)$  [1], influences the  $K_Q$  value determined.

The effect of  $K_f(\max)$ , the maximum stress intensity value used in the final stages of fatigue cracking on  $K_Q$ , was investigated and is reported in Table 2. The  $K_Q$  values were measured according to the general procedure outlined in ASTM E399 [1]. The friction at the loading pins was minimized by the use of flat bottom clevis and that at the clip gauge support was reduced by the use of razor blades. The load and secant value used to obtain  $K_Q$  were determined from Eq. (7), and the load and the displacements were recorded with an accuracy of  $\pm 0.25\%$ . The  $K_Q$  value was determined with an estimated accuracy of  $\pm 2\%$ .

As shown in Table 2,  $K_Q$  values can be significantly increased due to the crack closure that occurs when the plastic zone formed at the crack tip during fatigue cracking is unloaded. Obviously, the  $K_f(\max)$  value should be low, preferably below  $K_f(\max)/\sigma_Y\sqrt{W} < 0.22$  to ensure the absence of the effect of  $K_f(\max)$  on the determined  $K_Q$  values.

Considering the potential sources of error in the determination of  $K_Q$ , the agreement between the experimental and calculated values in Fig. 6 is good. The agreement implies that  $K_Q/\sigma_Y\sqrt{W}$  is a constant and is equal to 0.5. For convenience in future discussions, the calculated line in Fig. 6 is referred to as "line A." Thus, in the absence of crack growth,  $K_Q$  values measured correctly should fall on line A.  $K_Q$  values



measured in the presence of crack growth will be located to the right of line A.

It is obvious from Figs. 4, 5, and 6 that, as  $W$  increases at a given  $a/W$ ,  $K_Q$  will increase, but  $M$  will remain constant. Finally, at a critical  $W = W_C$ ,  $K_Q$  will approach the stress intensity value at which the crack starts extension,  $K_{IC}$ . This is termed as the fracture toughness of the material. Substitution of  $W = W_C$  and  $K_Q = K_{IC}$  in the relationship  $K_Q^2/\sigma_Y^2 W = 0.25$  gives  $W_C = 4K_{IC}^2/\sigma_Y^2$ . At  $W > W_C$ ,  $K_Q > K_{IC}$ , and the crack growth starts. At  $W < W_C$ , only the plastic zone grows as  $W$  increases. This can be represented by line A in Fig. 6.

#### R-CURVE APPROACH AT $W > W_C$

The contribution of a limited amount of crack growth to the deviation from linearity is evaluated from the analysis of a typical R-curve data [2]. The contribution is evaluated in two different cases:

- (a) crack growth in the absence of plasticity (where the crack extends abruptly such as in a Type III or II load-displacement test record [1]),
- and (b) crack growth together with the growth of the plastic zone (the case encountered in Type-I load displacement test record [1]).

#### Crack Growth in the Absence of Plasticity

Figure 7 is a schematic representation of a typical R-curve for a specimen with width  $W > W_C$ , where  $K_R$  is the stress intensity value corrected for plasticity for a given value of crack extension,  $\Delta a$ . The R-curve is a measure of the resistance of a material to crack growth. The  $K_R$  value for zero crack extension is equal to  $K_{IC}$ , the fracture toughness

defined in this paper. It is assumed that the R-curve for a limited amount of crack extension, that is,  $\Delta a/a \leq 0.02$ , can be represented by

$$\frac{K_R^2 - K_{IC}^2}{\sigma_Y^2} \propto \Delta a \quad (8)$$

The assumption in Eq. (8) has the following justifications: (a) the form of the equation is dimensionally homogeneous; (b) the R-curve can also be represented as a plot of the parameter  $G$  versus  $\Delta a$ , where  $G = K_R^2$ . For small amounts of crack extension, the relationship in Eq. (8) is a good approximation of the typical R-curve data represented in terms of  $G$  [25]; and (c) the term on the left-hand side of Eq. (8) is a measure of the increments in the energy dissipated after the crack growth starts and therefore should be related to the amount of crack extension,  $\Delta a$ .

At 2% crack extension,  $K_R = K_Q$ . Thus, Eq. (8) can be written as

$$\frac{K_Q^2 - K_{IC}^2}{\sigma_Y^2} \propto \Delta a \quad (9)$$

Dividing both sides by  $W_C$ , shown to be a property of the material, we obtain

$$\frac{K_Q^2 - K_{IC}^2}{\sigma_Y^2 W_C} \propto \frac{\Delta a}{W_C} \quad (10)$$

At  $\Delta a/a = 0.02$  and  $a/W = 0.5$ ,  $\Delta a = 0.01 W$ . In addition, as explained earlier, the crack extension will start at a point on line A (Fig. 6).

Therefore,  $K_{IC} = 0.25 \sigma_Y \sqrt{W_C}$ . Thus the substitution of these two conditions in Eq. (10) gives the following proportionality:

$$\frac{K_Q^2 - K_{IC}^2}{K_{IC}^2} \propto \frac{W}{W_c}$$

Differentiation of the above equation gives  $\partial(K_Q^2/K_{IC}^2)/\partial(W/W_c)$ . However, at  $\Delta a/a = 0.02$ ,  $K_Q = K$ , and  $\Delta a = 0.01 W$  since  $a/W = 0.5$ . Therefore,

$$\frac{\partial(K_Q^2/K_{IC}^2)}{\partial(W/W_c)} = 0.01 \left[ \frac{\partial(K^2/K_{IC}^2)}{\partial(\Delta a/W_c)} \right]_{\Delta a/a=0.02} \quad (11)$$

The term on the right-hand side of Eq. (11) can be evaluated, at any given values of  $K_{IC}$  and  $W_c$  and  $a/W$  ratio, from  $F$ , the standard  $K$  calibration factor for a given specimen geometry and  $a/W$  value, that is,

$$\left[ \frac{\partial(K^2/K_{IC}^2)}{\partial(\Delta a/W_c)} \right]_{\Delta a/a=0.02} = \left[ \frac{1}{F^2} \frac{\partial(F_{\Delta a}^2)}{\partial(\Delta a/W)} \right]_{\Delta a/a=0.02} \quad (12)$$

where  $F = KB\sqrt{W}/P$  and is a function of  $a/W$  only [26] and

$$F_{\Delta a} = F[(a + \Delta a)/W]$$

The  $K$  calibration factor,  $F$ , as a function of  $a/W$  is known [26]. Therefore, the term on the right-hand side in Eq. (12) can be evaluated numerically. The numerical calculations show that the term,  $1/F^2 \cdot \partial(F_{\Delta a}^2)/\partial(\Delta a/W)$  does not vary much, over a considerable range of crack growth, that is, at  $0 < \Delta a/a < 0.05$ . At  $a/W = 0.5$  and  $\Delta a/a = 0.02$ , this term has a value

$$\frac{1}{F^2} \frac{\partial(F_{\Delta a}^2)}{\partial(\Delta a/W)} = 6.4 \quad (13)$$

Substituting Eqs. (13) and (12) in (11) gives

$$\frac{\partial(K_Q^2/K_{IC}^2)}{\partial(W/W_c)} = 0.064 \quad (14)$$

The 2% crack extension in the absence of crack tip plasticity can therefore be represented by a straight line with a slope of 0.064 in the  $(K_Q/K_{IC})^2$  versus  $W/W_C$  space. This line is termed "line C" in Fig. 8. Line A from Fig. 6 is also shown in this figure. The slope of line A is 1 in Fig. 8 since  $(K_Q/K_{IC})^2 = (4K_Q^2)/(\sigma_Y^2 W_C)$ . The intersection of lines A and C gives  $K_{IC}$  of the material in a situation where crack extension occurs abruptly without any plasticity.

Two observations can be made from Fig. 8. First, the start of crack extension preceded by the growth of a plastic zone equivalent to  $\Delta a/a = 0.02$  results in approximately a 16-times decrease in slope in the  $(K_Q/K_{IC})^2$  versus  $W/W_C$  plot. Therefore, the point of crack initiation can be readily identified if the data were represented in such or an equivalent plot. However, if a Type-III load-displacement test record [1] is obtained during the test, plasticity preceding crack growth is less than  $\Delta a_p/a = 0.02$ ; in such a case, the decrease in slope in the load-displacement test record as a result of crack initiation would be quite drastic and the point of crack initiation can be readily identified. Second, line C is almost parallel to the x axis which represents W. This indicates that, in the case where the crack extension occurs abruptly, an increase in W has little effect on  $K_{IC}$  determined by the intersection of the line C and any other line A with an arbitrary slope value less than 1, in Fig. 8. Line A with a slope value less than 1 indicates that plastic zone preceding crack growth is less than an amount equivalent to  $\Delta a_p/a = 0.02$ . And this can occur in specimens with  $W > W_C$ . The above discussion agrees with the observation that  $K_{IC}$  is either independent

of the width or only mildly dependent on it, in the case where a Type-III load displacement test record is obtained.

However, it must be noted that, during fracture toughness testing, quite often the crack grows together with the growth of plastic zone. We have to consider, therefore, the simultaneous growth of the crack and the plastic zone. This is done presently.

#### Crack Growth in the Presence of Plasticity

In the case where the crack grows together with the plastic zone, the total deviation from linearity,  $\Delta V/V$ , consists of two terms:

- (a) the term  $\Delta V_p/V_e$  that results from plastic zone growth; and
- (b) the term  $\Delta V_c/V_e$  that results from crack growth. These terms were earlier defined in Fig. 3:

$$\frac{\Delta V}{V_e} = \frac{\Delta V_p}{V_e} + \frac{\Delta V_c}{V_e} \quad (15)$$

The relationship between  $\Delta V_p/V_e$  versus  $K^2/\sigma_Y^2 W$  was shown earlier in Fig. 4. At  $\Delta a/a = 0.02$ ,  $K = K_Q$ ; therefore the relationship can be approximately represented by

$$\frac{\Delta V_p}{V_e} = 0.2 \frac{K_Q^2}{\sigma_Y^2 W} \quad \text{for } a/w = 0.5 \quad (16)$$

The contribution of crack extension to the deviation from linearity is calculated from the standard compliance relationship in a manner described earlier in Eqs. (5), (6), and (7). Accordingly,

$$\frac{\Delta V_c}{V_e} = \frac{f'}{f} \frac{\Delta a_c}{W}$$

At  $a/W = 0.5$ ,  $f/f'$  can be evaluated from the reported compliance relationship  $EVB/P = f$  as a function of  $a/W$  [24]. At  $a/W = 0.5$ ,  $f'/f = 5$ . Therefore, the above equation reduces to

$$\frac{\Delta V_c}{V_e} = 5 \frac{\Delta a_c}{W} \quad (17)$$

It was earlier indicated that the slope, as given in Eq. (13), does not change much with  $\Delta a/W$ . Besides, at  $\Delta a/a = 0.02$ ,  $K = K_Q$ ; one can then write

$$\frac{\Delta a_c}{W} = \frac{K_Q^2}{\sigma_Y^2 W} \left/ \frac{\partial (K^2/\sigma_Y^2 W)}{\partial (\Delta a/W)} \right. = \frac{K_Q^2}{6.4 \sigma_Y^2 W} \text{ at } a/W = 0.5 \quad (18)$$

Substitute Eqs. (18), (17), and (16) into (15) and solve for  $K_Q^2/\sigma_Y^2 W$ .

One then gets

$$K_Q^2/\sigma_Y^2 = 0.051 W \quad (19)$$

Divide Eq. (19) by  $0.25 W_C$  and obtain

$$\frac{K_Q^2}{K_{IC}^2} = 0.204 \left( \frac{W}{W_C} \right) \quad (20)$$

Thus, the combined effect of the crack growth and the plastic zone can be represented as straight lines with slopes equal to 0.051 in a  $K_Q^2/\sigma_Y^2$  versus  $W$  plot and 0.204 in a  $K_Q^2/K_{IC}^2$  versus  $W/W_C$  plot. For convenience, these lines are referred to as line B.

## DISCUSSION

### Comparison of Experimental and Calculated Results

The  $K_Q$  or  $K_{IC}$  values have been determined in the CT specimens for different combinations of progressively increasing widths and thicknesses prepared from titanium alloys [4] and an aluminum alloy [6]. The

experimental and the calculated values of the parameter  $K_Q^2/\sigma_Y^2W$  are compared in Fig. 9.

The experimental  $K_Q$  or  $K_{IC}$  values fall around the computed lines A and B. This has some interesting implications. Some of the experimental data points lie to the left of line A. The reason for such scatter in the experimental data has been explained earlier during the discussion of Fig. 6. Generally, the agreement between the experimental data and the calculated line B is quite good. The reasonably limited scatter around the line A and the good agreement of the experimental data with line B is particularly striking when one considers that the experimental data were obtained with specimens whose thickness varies by almost one order with the  $B/(K_Q/\sigma_Y)^2$  value ranging approximately from 0.5 to 5. If the constraint were to depend on the thickness as assumed in ASTM E399,  $K_Q$  should change significantly with thickness.

It should be noted that the intersection of lines A and B gives a  $K_Q$  value equal to  $K_{IC}$  of the material.

The results of the analyses presented in this paper predicts that, in a  $(K_Q/K_{IC})^2$  versus  $W/W_C$  space, the experimental data point for all materials should fall around a single B line. Accordingly, the experimental data points located close to the B lines in Fig. 9 are replotted in Fig. 10. The experimental data, obtained from materials with different  $K_{IC}$  and  $\sigma_Y$ , give results that fall around a single line B. The agreement indicates that the analyses of the width dependence of toughness and the assumptions made in the present paper are essentially correct. As pointed out earlier, this agreement is all the

more notable when one considers that the data obtained from the specimens have thicknesses that vary widely.

#### A New Approach to the Determination of $K_{IC}$

As indicated earlier,  $K_{IC}$  in the present approach is defined as the stress intensity value at which the crack extension starts. Since the start of crack extension being considered in this paper is that which satisfies ASTM E399 requirements, this will be preceded by a very limited amount of plasticity and strain at the crack tip. Therefore, the start of the crack extension would be stress-induced. The fundamental basis of fracture toughness in such a case is outlined in Fig. 11 and discussed below. After that, the new approach to the determination of  $K_{IC}$ , which is consistent with the fundamental basis of fracture toughness, is outlined.

The stress intensity factor is given by

$$K = \sigma_{yy} \sqrt{2\pi} \quad \text{at} \quad r \ll a \quad (21)$$

where  $\sigma_{yy}$  is the local normal stress at the crack tip in the plane of fracture and  $r$  is the distance measured from the crack tip (as shown in Fig. 11). When the width is large and the plasticity is limited, the  $\epsilon_{yy} \propto 1/\sqrt{r}$  assumed in the analysis earlier, is nearly equivalent to  $1/\sqrt{r}$  stress distribution assumed in Eq. (21). If the width is small, the strains near the crack tip and the plastic zone is large and this decreases the yielding constraint at a given value of  $K$ .

At crack initiation,  $\sigma_{yy} \rightarrow \sigma_{yy}^*$  at  $r = r^*$  (see Fig. 11) and, correspondingly,  $K = K_{IC} = \sigma_{yy}^* \sqrt{2\pi r^*}$  where  $\sigma_{yy}^*$  and  $r^*$  depend on the strength and the microstructure of the material. A material has a



well-defined and reproducible fracture toughness if  $\sigma_{yy}^*$  and  $r^*$  have clearly defined values.

$K_{IC}$  defined above depends on the magnitude of  $\sigma_{yy}$  at  $r = r^*$  and this, in turn, depends on the yielding constraint. Thus, to obtain a reproducible  $K_{IC}$  value in a material, the  $K_{IC}$  should be measured in a situation where the yielding constraint is above a certain minimum value. The minimum value of  $M$  is probably about 3.

The results presented in the earlier sections can be used to evolve a new approach to the determination of the  $K_{IC}$  as defined above. It is shown in Fig. 5 that the constraint to crack tip yielding increases with the width of a CT specimen. If the width is sufficiently large, that is,  $W > W_C$ , a so-called plane strain fracture under high yielding constraint can be produced. It is also shown from a combined consideration of Figs. 4 and 5 that all points on line A have a constant value of  $M$  for a given  $a/W$ . At  $W < W_C$ ,  $K_Q^2 \propto W$  and the 5% secant deviation from linearity is produced only by the growth of the plastic zone and gives rise to line A as shown in Fig. 6. At  $W = W_C$ , the crack growth starts and  $K_Q = K_{IC}$ . This is consistent with the definition of  $K_{IC}$  as outlined in Fig. 11. At  $W > W_C$ , the deviation from linearity is produced by the growth of the plastic zone as well as the crack. The analysis, which evaluates the relative contribution of the growth of plastic zone and the crack to the total deviation from linearity and produces the line B, is shown to be essentially correct in Figs. 9 and 10. Based on these observations, the new approach to the determination of  $K_{IC}$  is outlined below.

First, draw line A, with a slope of 0.25, in the  $K_Q^2/\sigma_Y^2$  versus  $W$  space as shown in Fig. 12. Measure  $K_Q$  in a compact tension specimen with  $W > 4(\sigma_Q/\sigma_Y)^2 = W_C$  and  $a/W = 0.5$ , following a procedure identical to that in ASTM E399. Next, locate the measured  $K_Q$  value in Fig. 12. The  $K_Q$  value is indicated by the point marked "X". Then, draw a line B with slope  $\approx 0.05$  through the point X. The intersection of lines A and B gives a  $K_Q$  value equal to  $K_{IC}$ . The approach as outlined above applies to the case where a Type-I load-displacement test record is obtain

The operational definition of  $[K_{IC}]_{399}$  is based on 2% crack extension. This is different from the  $K_{IC}$  as defined in Fig. 11. In most instances,  $[K_{IC}]_{399}$  will be higher than the  $K_{IC}$  as defined here. Table 3 compares the  $K_{IC}$  as defined here and  $[K_{IC}]_{399}$  for some of the materials investigated by other workers [4,6].

#### Growth of the Plastic Zone and the Crack in the Three Cases

During fracture toughness testing of specimens with width  $W > W_C$ , the plastic zone can grow in three possible sequences: (a) the plastic zone grows only before the 2% crack extension; (b) the plastic zone grows both before and during the 2% crack extension; and (c) the plastic zone grows only after the 2% crack extension. These three possible cases which can be encountered during the testing are discussed below. In the testing situation where  $W < W_C$ ,  $K_Q$  values obtained by the secant technique will lie on line A.

Case 1. In this case, the plastic zone grows only before the 2% crack extension. During the 2% crack extension, the growth of plastic zone is negligible. The Types II and III load-displacement test records

[1] which exhibit abrupt start of crack extension are usually observed in this case. The value of  $K_{IC}$  can be obtained by the intersection of line A and the line C which has a slope = 0.016 in the  $(K_Q/\sigma_Y)$  vs  $W$  plot. However, since the plasticity preceding crack extension may be less than 2%, the  $K_{IC}$  is more appropriately determined in this case, following the procedure described in ASTM E399. The two procedures will yield, though, only marginally different  $K_{IC}$  values. In the limiting case where the plastic zone grows by an amount equivalent to 2% crack extension prior to the abrupt physical crack extension, the  $K_{IC}$  value can be obtained by the intersection of lines A and C.

Case 2. In this case, the plastic zone grows before as well as during the 2% crack extension. In such a case, usually a Type-I load-displacement test record [1] is obtained. The experimental data on line B in Figs. 9 and 10 belong to this case and  $K_{IC}$  is obtained by the intersection of the lines A and B as shown in Fig. 12.

Case 3. The plastic zone does not grow before but does so only after the start of crack extension. Obviously, this situation is physically improbable and is therefore a hypothetical case. However, the  $K_{IC}$  in this case should be obtained by the intersection of line B with the  $x$  axis. For a finite  $K_Q$  value, such an intersection occurs at a negative critical width,  $W_C$  value, and therefore has no physical significance.

#### Comments on the Approach

The approach is simple, straightforward, and is identical to ASTM E399 in terms of the procedure of measurement.

The procedure as outlined above can be used to determine the toughness in a compact tension specimen with crack lengths different from  $a/W = 0.5$ . However, line B in that case will have a different slope. The analysis to determine lines A, B, and C has also been made for three-point bend and single-edge notched tension specimens. The general trend of the results for the three different specimens is similar; however, the slopes of the lines are different in the three different specimens.

The toughness measured here is based on the growth of the plastic zone equivalent to 2% crack extension. This is done for several reasons. First, it is consistent with E399 procedure. Second, if the plastic zones were larger than the 2% equivalent crack extension, the domination of the  $1/\sqrt{r}$  singularity implicitly assumed in the definition of  $K$  may be in considerable error. Besides, a large plastic zone may lower the yielding constraint too much to produce a stress-induced plane strain fracture. Finally, if the toughness were to be based on plastic zone sizes smaller than 2% equivalent crack extension, an accurate determination of  $K_Q$  would be difficult because, in such a case, the corresponding  $\Delta V_p/V$  or the secant values will be smaller than that given in Table 1. It can be seen from Fig. 4 that, initially,  $K/\sigma_y \sqrt{W}$  rises sharply with  $\Delta V_p/V$ ; therefore, when the secant or the  $\Delta V_p/V$  value is small, the experimental  $K_Q$  values measured can be in considerable error due to a small error in the secant measurement.

It should also be noted that it is possible to measure  $K_{IC}$  in a specimen with  $W < W_C$  through a plasticity corrected  $K$  value (as in the R-curve approach) provided the crack initiation is identified by an independent technique.

The approach to the determination of  $K_{IC}$  as presented here has several advantages. First, it gives a  $K_{IC}$  value that is independent of the width and also of the thickness of the specimen. The  $K_{IC}$  as defined in this approach is consistent with  $J_{IC}$  and R-curve approach since all of them are based on the start of crack growth. Finally, the approach recognizes that a crack can extend under linear elastic conditions in thin and wide plates and therefore the determination of  $K_{IC}$  in such plates is possible. Obviously, this increases the range of applicability of the  $K_I$ - $K_{IC}$  approach to a wider combination of materials and configurations.

#### Implication of the Results

The agreement between the experimental data obtained from specimens with widely varying thicknesses and the predicted results in Figs. 9 and 10 indicates that the growth of the plastic zone before and during the crack extension is not significantly influenced by the thickness of a compact tension specimen. On the other hand, in the compact tension specimen, the plasticity depends significantly on the width. The width dependence of plasticity, however, depends on the specimen configuration: for example, the analysis reported here shows that in single-edge notch tension specimens, the width dependence of plasticity is significantly less than that in a compact tension specimen. In a center notch specimen, where the stress gradient over the whole ligament along the direction of the crack is smaller, the width dependence of plasticity is expected to be even less. A precise, three-dimensional, elastic-plastic, finite-element analysis is required to understand the relative contribution of

the width and the thickness of a configuration to the limited plasticity effects. Alternatively, the elastic and the plastic part of the thickness direction contraction as dependent on the thickness, width and configuration needs to be experimentally determined.

The loading of a thin, as against a thick, structure or specimen often produces an out-of-plane bending, and this can obscure the experimentally observed relative effects of width and thickness on the plasticity. Such bending can produce a significant amount of loading in the Mode III at the crack tip. The growth of the plastic zone at the crack tip under Mode III shear stress is quite different from the situation where it is absent. In fact, the use of guide plates has considerable effect on the experimental  $K_Q$  values of thin specimens. So long as buckling and out-of-plane bending of the specimen or the structure can be avoided, the width is expected to exert a relatively large influence on the plasticity and constraint in a given configuration.

The width dependence of the constraint, as shown in Fig. 5, implies that the start of the growth of a crack in a thin but wide structure can occur under linear elastic condition. Thus, a  $K$  approach would be adequate to characterize fracture in such a situation. This is, of course, done at present through the R-curve approach. A  $J$  approach will be significant only with the width dimension  $W < W_C$ .

It may also be noted that, in the usual representation of fatigue crack growth, according to Paris convention, the start of stage-III crack growth is associated with the onset of considerable plasticity. The width dependence of constraint shows that the linear elastic behavior in a wider structure is extended to a higher  $K$  value. Therefore,

in a wider specimen or structure, the stage-II fatigue crack growth behavior will be extended to a higher  $\Delta K$  versus  $da/dN$  regime, where  $\Delta K$  is the range of stress intensity factor and  $da/dN$  is the increment in crack length per cycle during fatigue loading. This has significant ramifications with regard to the prediction of the behavior of the structure from the data obtained from the small specimens, particularly under spectrum loading.

In testing of materials, a specimen of lower thickness, but larger width, may be tested to achieve a high constraint and to obtain a valid  $K_{IC}$  value. Since  $P_Q$  increases directly with  $B$ , but increases only with the square root of  $W$ , a thin but wide specimen will require a machine with smaller capacity and yet meet the constraint requirement for valid  $K_{IC}$  measurement. However, adequate care must be taken to meet the problems of alignment and buckling encountered during the testing of wide specimens.

#### SUMMARY AND CONCLUSIONS

1. A method of determination of  $K_{IC}$  is proposed and is verified by comparing experimental and calculated results.
2. The method gives a  $K_{IC}$  value that is independent of width.
3. The  $K_{IC}$  value determined is defined on the basis of the start of crack extension and is therefore consistent with the R-curve and  $J_{IC}$  approaches.
4. The approach enables one to determine  $K_{IC}$  in thin but wide plates, and therefore increases the range of applicability of the  $K - K_{IC}$  approach to a wider combination of materials and configurations.

## REFERENCES

- [1] ASTM E399, 1976 Annual Book of ASTM Standards, p. 471.
- [2] ASTM STP 632, "R-Curve Determination, ASTM Standards Designation, E561-76T," in Development in Fracture Mechanics Test Methods Standardization, 1977, p. 241.
- [3] Munz, D., "Minimum Specimen Size for the Application of Linear Elastic Fracture Mechanics," paper presented at ASTM Symposium Elastic-Plastic Fracture, November 16-18, 1977, Atlanta, Georgia.
- [4] Munz, D., Galda, K. H., and Link, F., in Mechanics of Crack Growth, ASTM STP 590, 1975, p. 219.
- [5] Kaufman, J. G., in Development in Fracture Mechanics Test Methods Standardization, ASTM STP 632, 1977, p. 3.
- [6] Kaufman, J. G. and Nelson, F. G., in Fracture Toughness and Slow Stable Crack Growth, ASTM STP 559, 1974, p. 74.
- [7] Lake, R. L., in Mechanics of Crack Growth, ASTM STP 590, 1976, p. 208.
- [8] Wang, D. Y. and McCabe, D. E., in Mechanics of Crack Growth, ASTM STP 560, 1975, p. 169.
- [9] Jones, M. H. and Brown, W. F., in Review of Developments in Plane Strain Fracture Toughness Testing, ASTM STP 463, 1970, p. 63.
- [10] Newman, J. C., Jr., in Properties Related to Fracture Toughness, ASTM STP 605, 1976, p. 104.
- [11] Paranjpe, S. A. and Banerjee, S., "Fracture," Fourth International Conference, University of Waterloo, Canada, Vol. 3, 1977, p. 343.
- [12] Paranjpe, S. A. and Banerjee, S., Engineering Fracture Mechanics, Vol. 10, 1978, p. 583.



- [13] Paranjpe, S. A., "Interrelation of Crack Opening Displacement with Stress Intensity Factor and J Integral," Ph.D. Thesis, Indian Institute of Technology, Bombay, 1976.
- [14] Dixon, J. R., Strannigen, J. S., and McGregor, J., J. Strain Anal., Vol. 4, 1969, p. 27.
- [15] Gerberich, W. W., Experimental Mech., Vol. 2, 1961, p. 335.
- [16] Ke, J. S. and Liu, H. W., Eng. Fract. Mech., Vol. 5, 1973, p. 187.
- [17] Ewing, D. J. F. and Richards, E. E., J. Mech. Phys. Solids, Vol. 22, 1974, p. 27.
- [18] Merkle, J. G. and Corten, H. T., J. Pressure Vessel Tech., Paper 74-PVP-33, 1975.
- [19] Paranjpe, S. A., Ph.D. Thesis, Indian Institute of Technology, Bombay, India, 1976.
- [20] Brown, K. M., SIAM Journal on Numerical Analysis, Vol. 6(4), 1969, p. 560.
- [21] Rice, J. R. and Johnson, M. A., in Inelastic Behavior of Solids, M. F. Kamminen, et al., Eds., McGraw Hill, New York, 1970, p. 641.
- [22] McClintock, F. A. and Irwin, G. R., in Fracture Toughness Testing and Its Application, ASTM STP 381, 1965, p. 84.
- [23] Irwin, G. R., Appl. Mater. Res., Vol. 3(6), 1964, p. 65.
- [24] McCabe, D. E. and Sha, G. T., in Fracture Mechanics Test Methods Standardization, ASTM STP 632, 1977, p. 82.
- [25] Heyer, R. H., in Fracture Toughness Evaluation by R-Curve Methods, ASTM STP 527, 1973, p. 1.
- [26] Newman, J. C., Jr., in Fracture Analysis, ASTM STP 560, 1974, p. 105.

TABLE 1—Deviation from linearity ( $\Delta V_p/V$ ) due to the growth  
of plastic zone equivalent to 2% crack extension  
( $\Delta a/a = 0.02$ ) in CT specimens.

a/W	$\Delta V_p/V_e$ for $\Delta a_p/a = 0.02$	$K_Q^1/\sigma_Y\sqrt{W}$
	from Eq. (7)	from Eq. (7) and Fig. 4
0.4	0.038	0.52
.5	.050	.5
.6	.069	.5

$K_Q^1$  is defined as the stress intensity factor corresponding to 2% crack extension as measured by the secant technique. In the absence of physical crack extension, the 2% crack extension corresponds to  $\Delta a/a = \Delta a_p/a = 0.02$ .

TABLE 2—Dependence of experimentally determined  $K_Q$  on  $K_f(\max)$ <sup>1</sup>  
in a 1CT specimen prepared from ASTM 516-grade 70 steel;

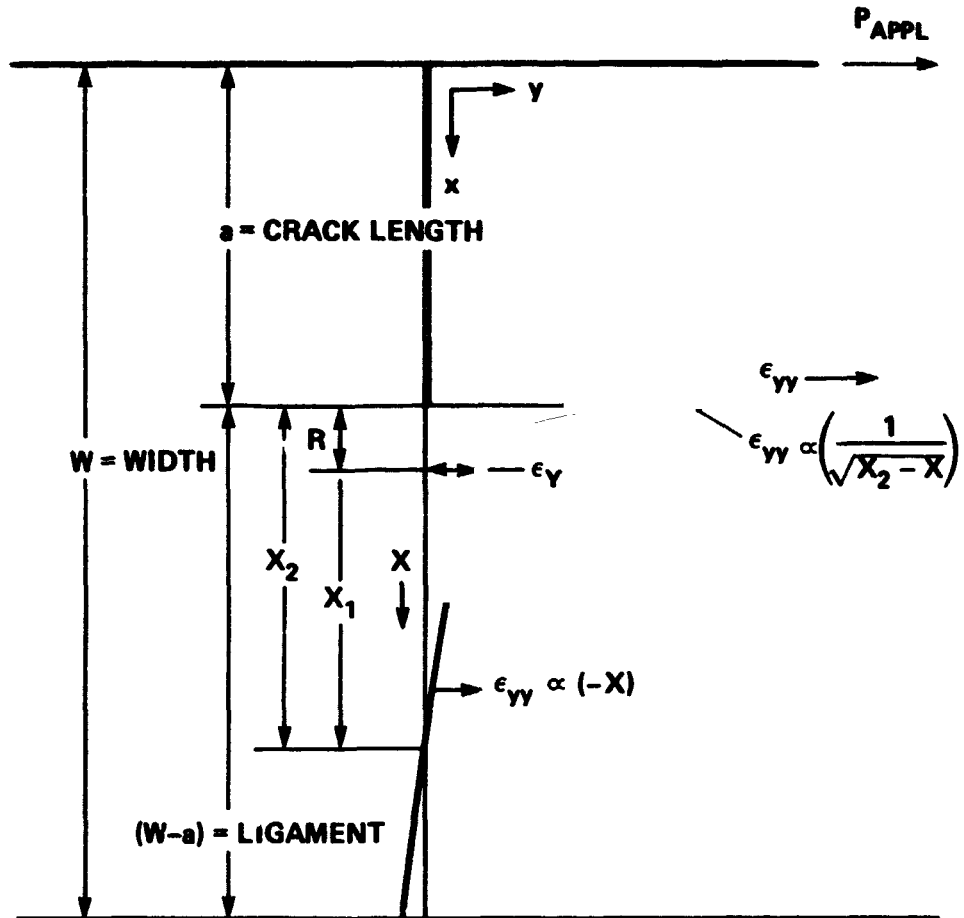
$\sigma_Y = 47$  Ksi.

a/W	$K_Q$ , Ksi $\sqrt{\text{in.}}$	$K_f(\max)$ , Ksi $\sqrt{\text{in.}}$	$K_Q/\sigma_Y\sqrt{W}$	$K_f(\max)/\sigma_Y\sqrt{W}$
0.402	36	16	0.54	0.24
0.501	35	17.2	0.52	0.25
0.507	34	16	0.51	0.24
0.661	37	20	0.55	0.30
0.652	44	27	0.66	0.40
0.667	47	30	0.70	0.45
0.570	49	32	0.73	0.48

<sup>1</sup>  
 $K_f(\max)$  is the maximum value of the stress intensity used  
during the final stages of fatigue cracking.

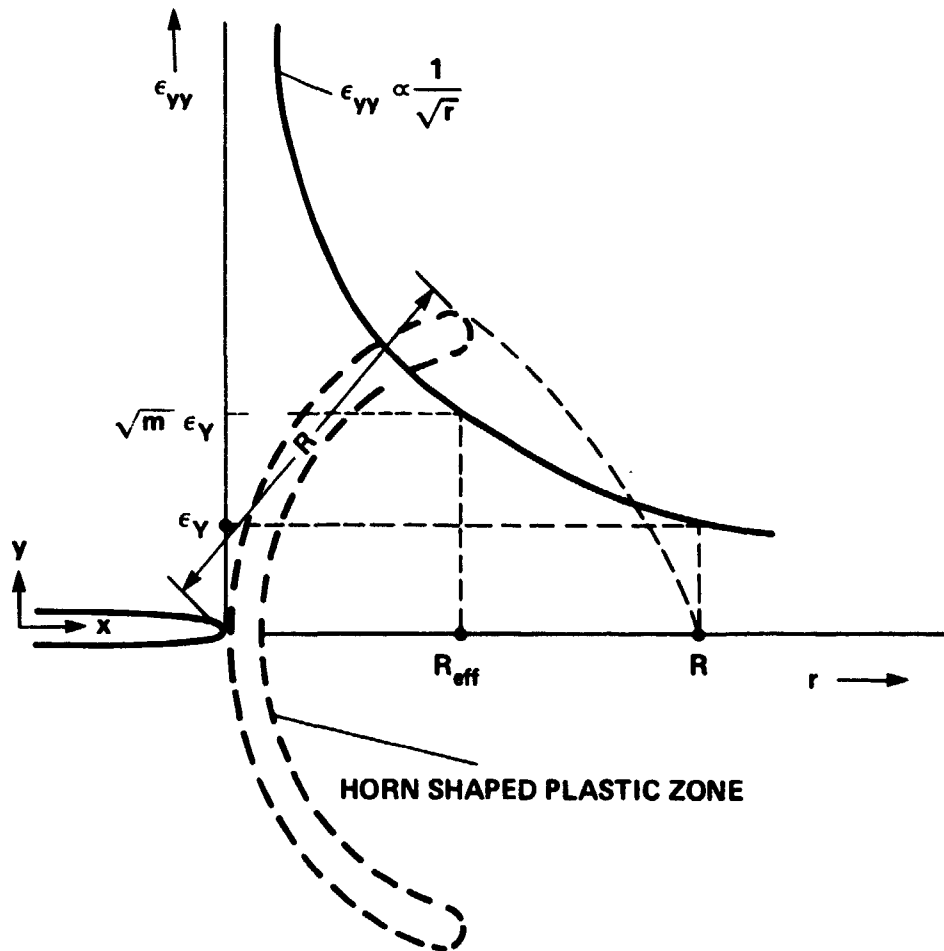
TABLE 3—Comparison of  $[K_{IC}]_{399}$  with  $K_{IC}$  determined by  
the intersection of lines A and B.

Reference	Material	$[K_{IC}]_{399}$	$K_{IC}$
[3]	Ti-6Al-4V- Plate A	82-92 MNm <sup>-3/2</sup>	77 MNm <sup>-3/2</sup>
[3]	Ti-6Al-4V- Plate B	---	69 MNm <sup>-3/2</sup>
[5]	2219-T851 Al-Alloy	35.5 Ksi√in.	29 Ksi√in.



NOTE: IN THE ANALYSIS, THE ORIGIN OF THE ORDINATE IS TAKEN AT THE POSITION OF THE STRAIN REVERSAL POINT. ACCORDINGLY,  $r$ , THE DISTANCE FROM THE CRACK TIP  $= X_2 - X$ .

FIG. 1 - Strain distribution in the ligament,  $(W-a)$ , of a compact tension specimen.



NOTE:  $m$  IS A MEASURE OF THE YIELDING CONSTRAINT, AND IS DEFINED IN EQUATION (2). AS SHOWN IN FIGURE 1, THE STRESS  $\epsilon_{yy} \propto 1/\sqrt{r}$ .

FIG. 2 — The effective and the nominal plastic zone sizes in plane strain condition.



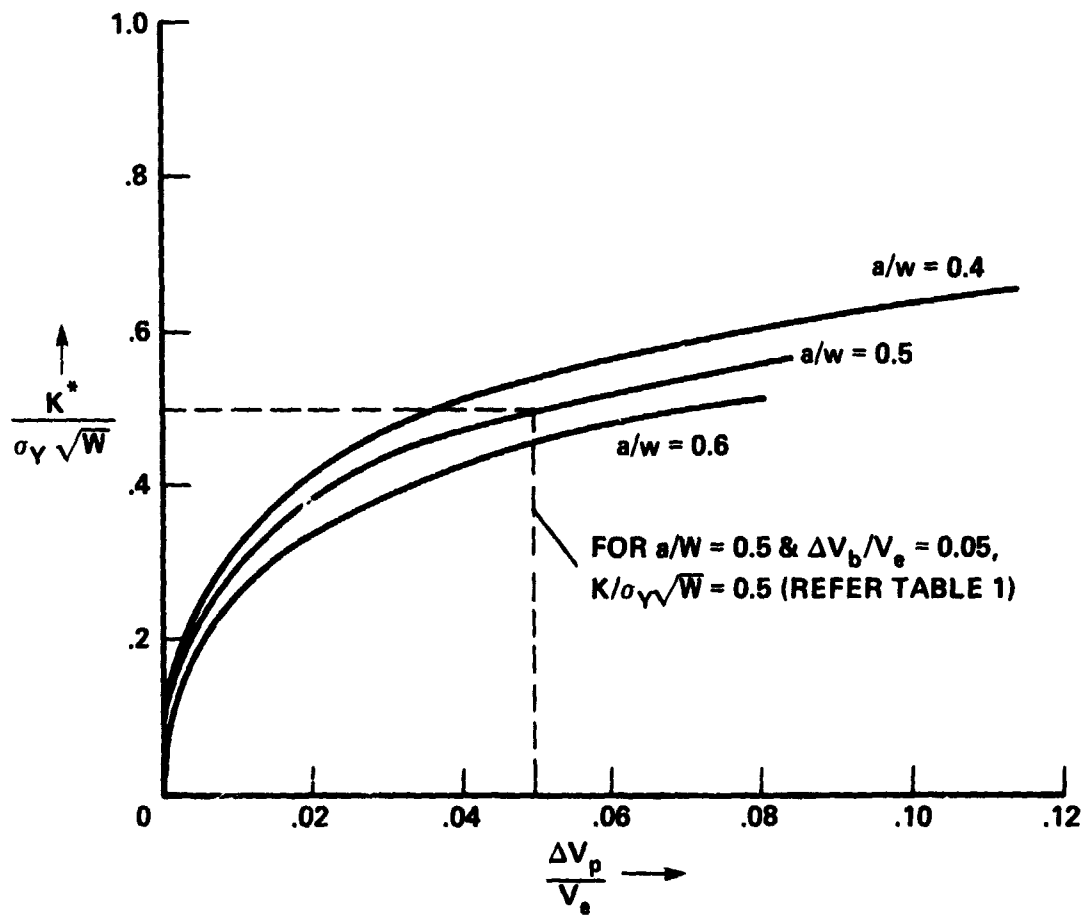


FIG. 4 - The parameter  $K/\sigma_Y \sqrt{W}$  as a function of the ratio  $\Delta V_p/V_e$ , a measure of the deviation from linearity due to the formation of plastic zone.



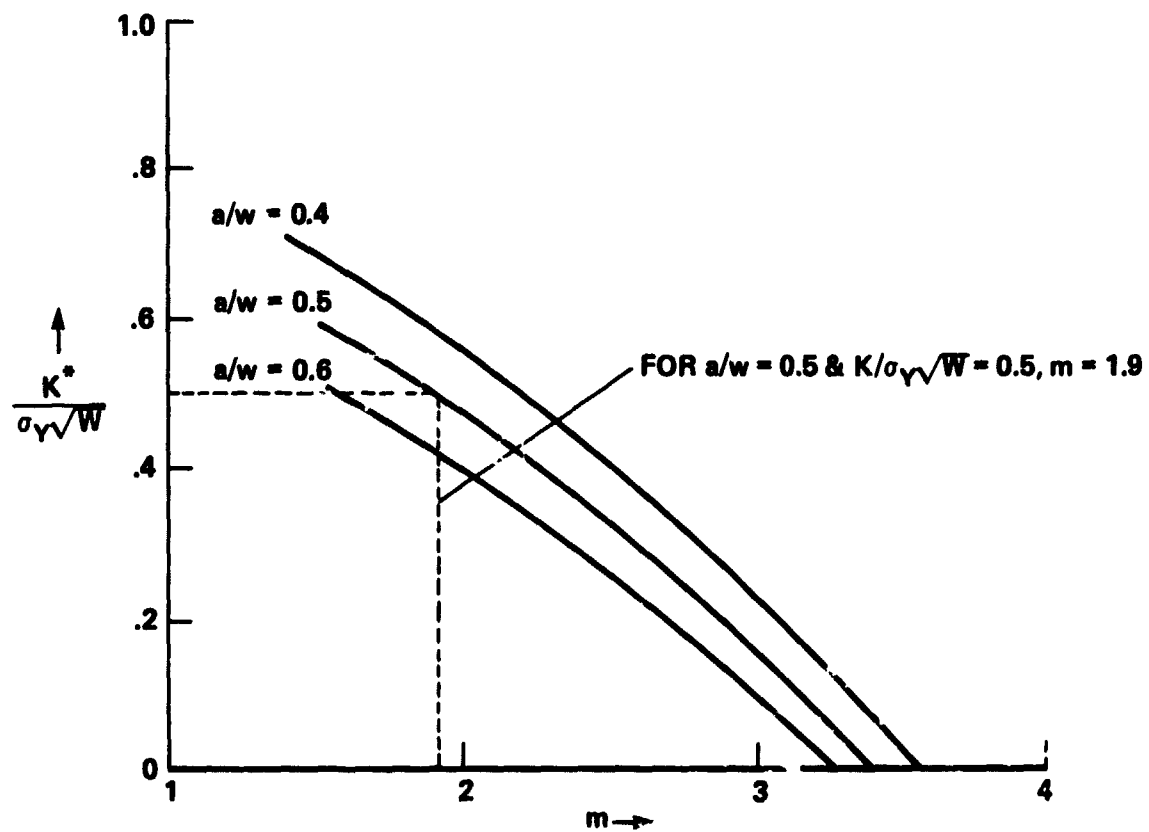


FIG. 5 — The parameter  $K/\sigma_Y \sqrt{W}$  as a function of the yielding constraint,  $m$ , for compact tension specimen with different values of  $a/W$ .

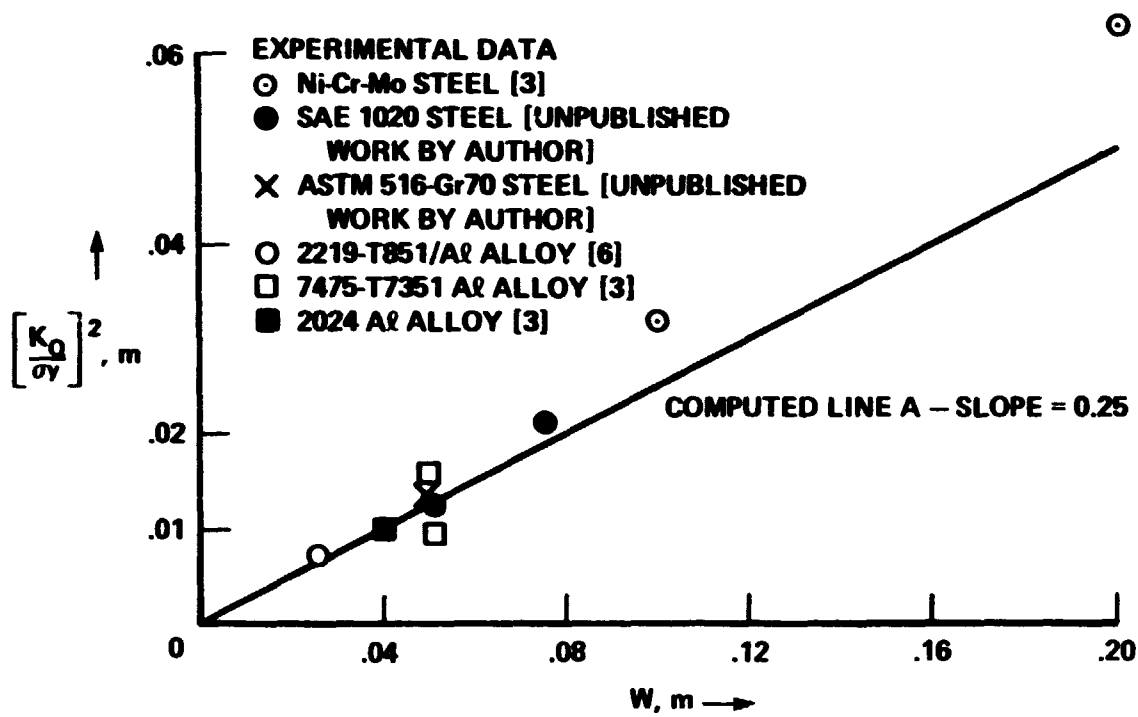


FIG. 6 - Calculated and experimental values of the parameter  $K_Q/\sigma_Y\sqrt{W}$ .

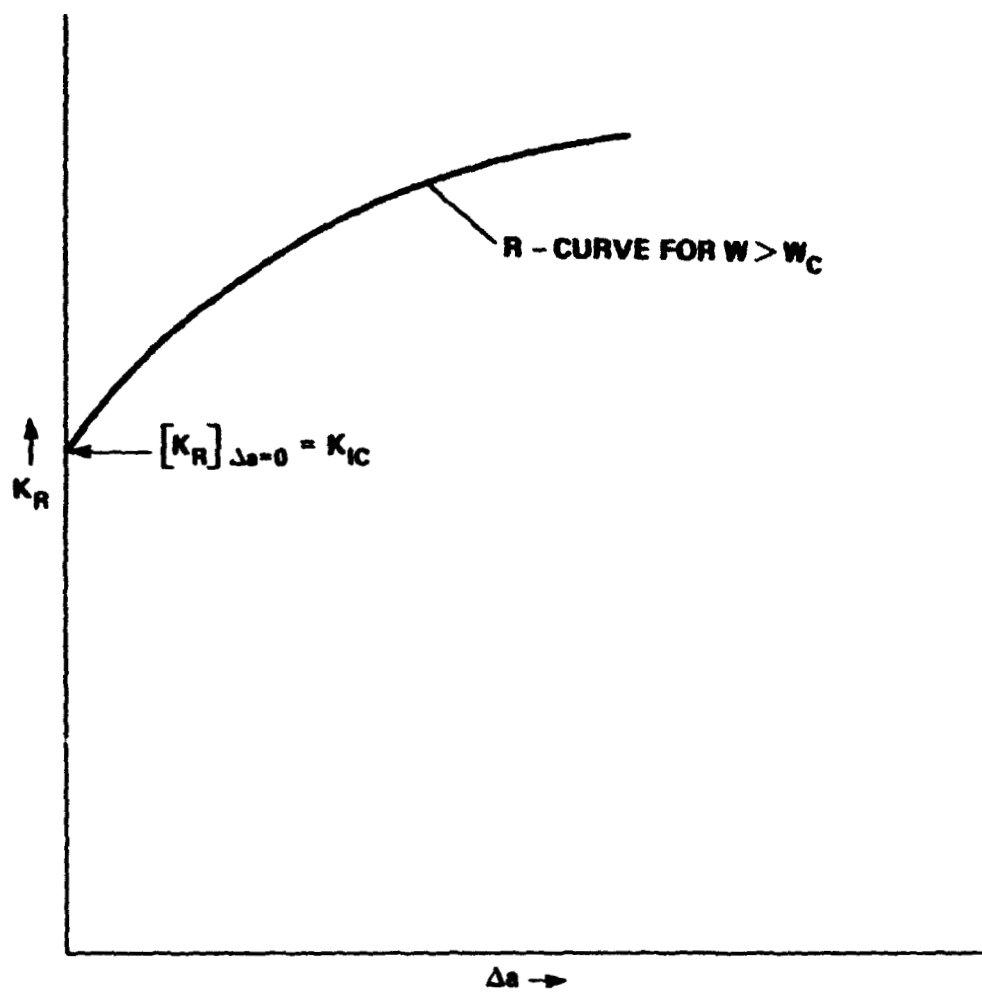


FIG. 7 - Schematic of a typical R curve for  $W > W_c$ .

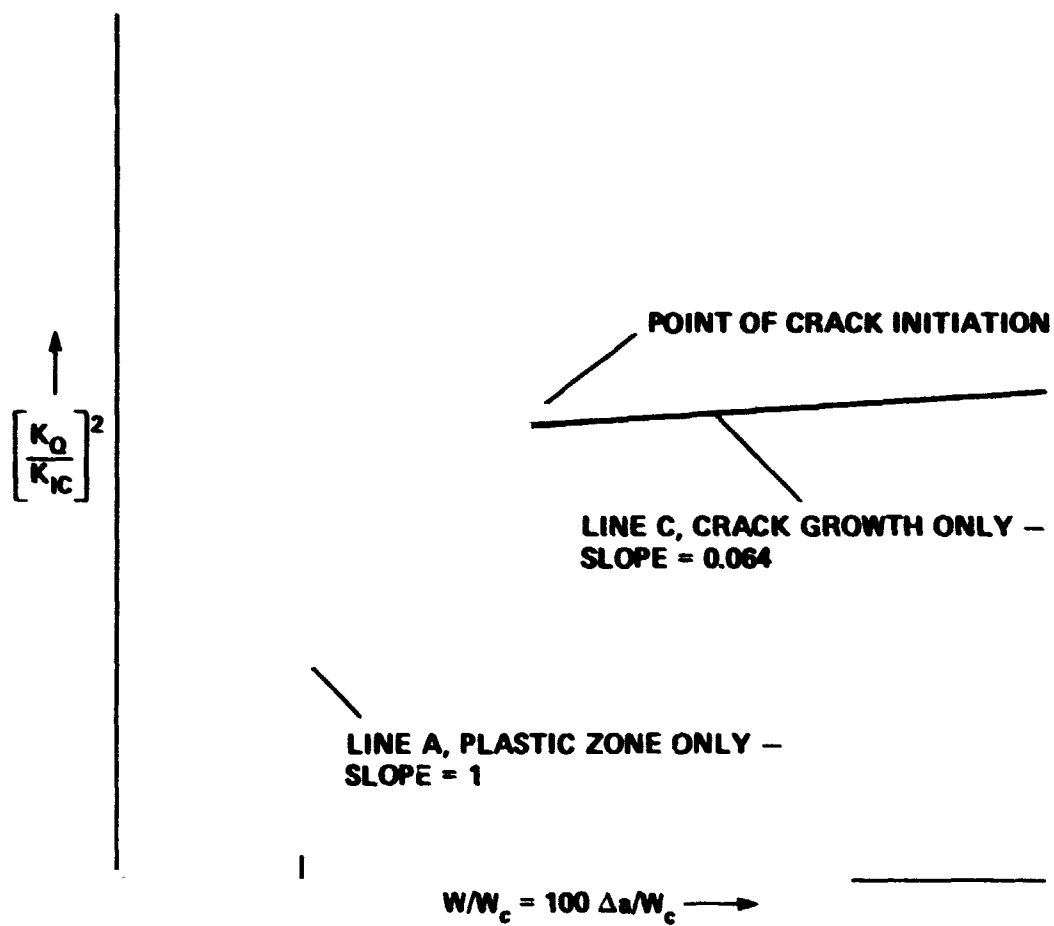


FIG. 8 - Schematic representation of crack growth in the absence of plasticity in a CT specimen with  $a/W = 0.5$ .

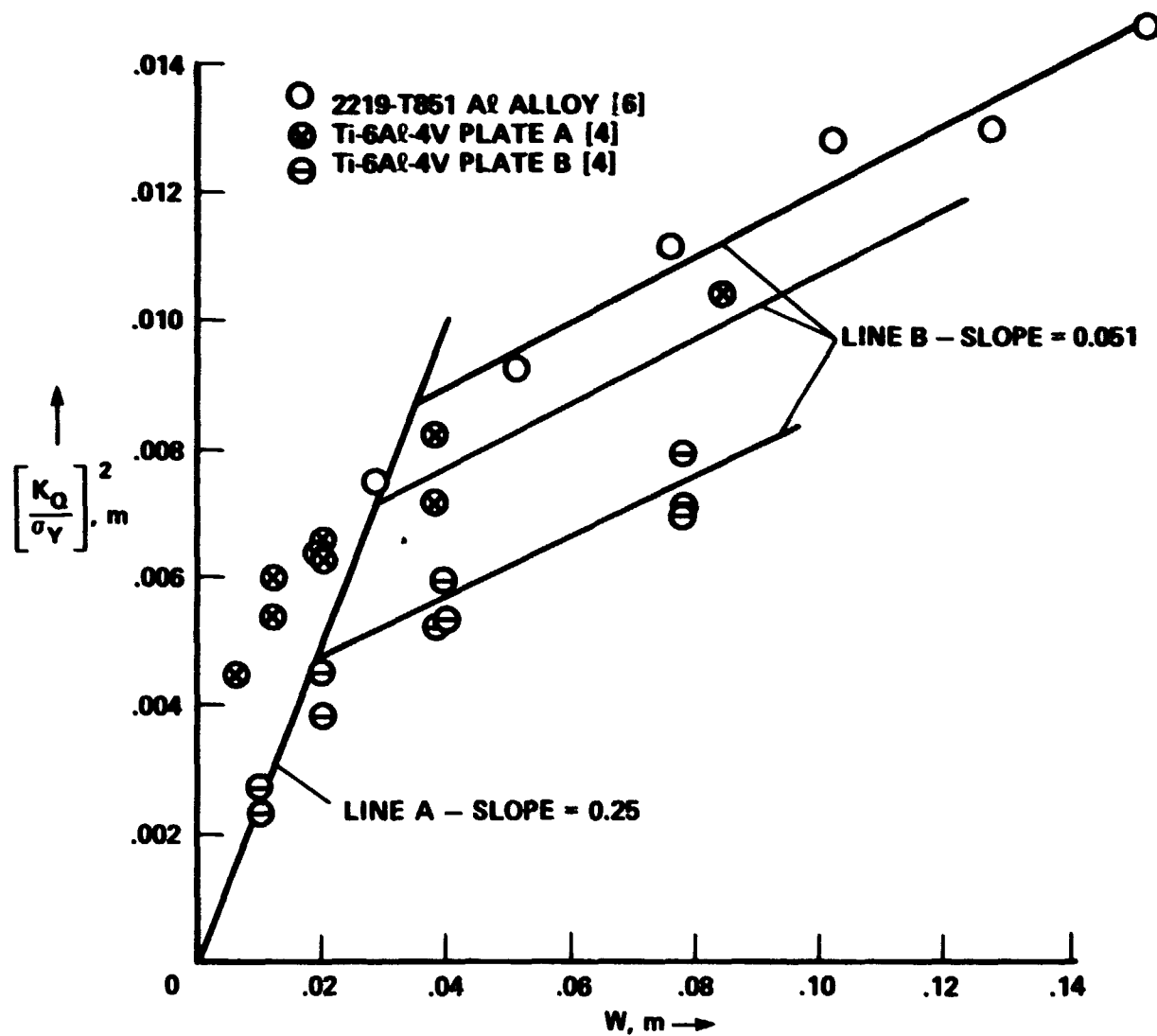


FIG. 9 - Experimental and predicted results in the  $(K_Q/\sigma_Y)^2$  versus  $W$  plots.

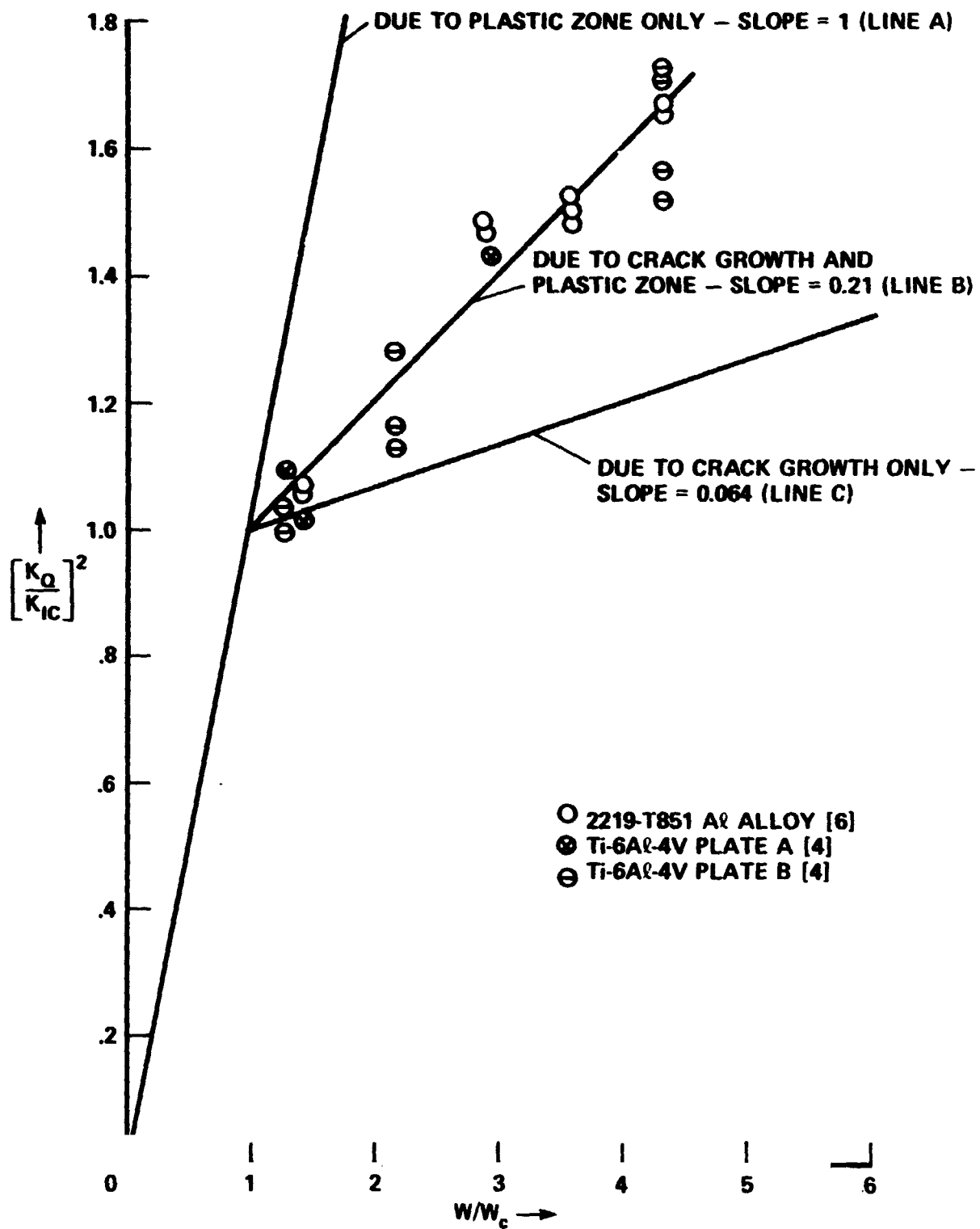


FIG. 10 - Experimental and predicted results in the  $(K_Q/K_{IC})^2$  versus  $W/W_c$  plots.

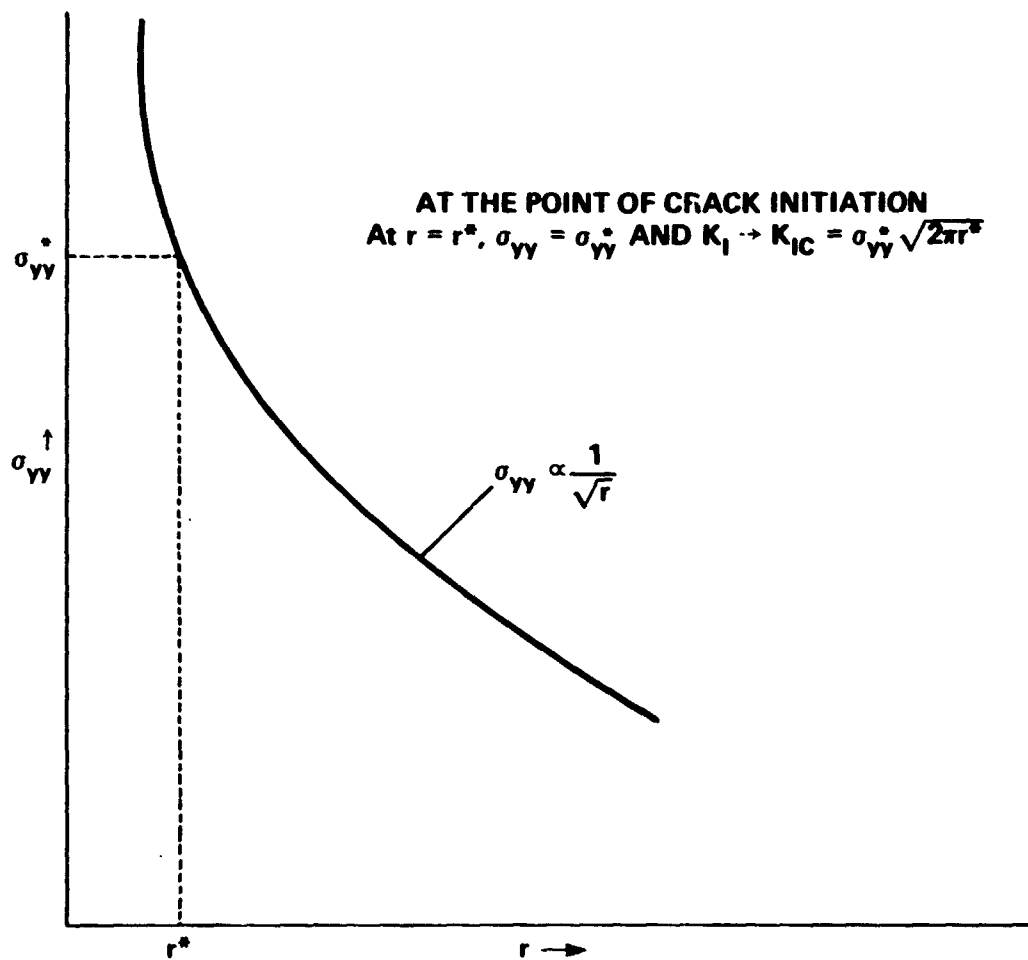


FIG. 11 — Definition of  $K_{IC}$ .

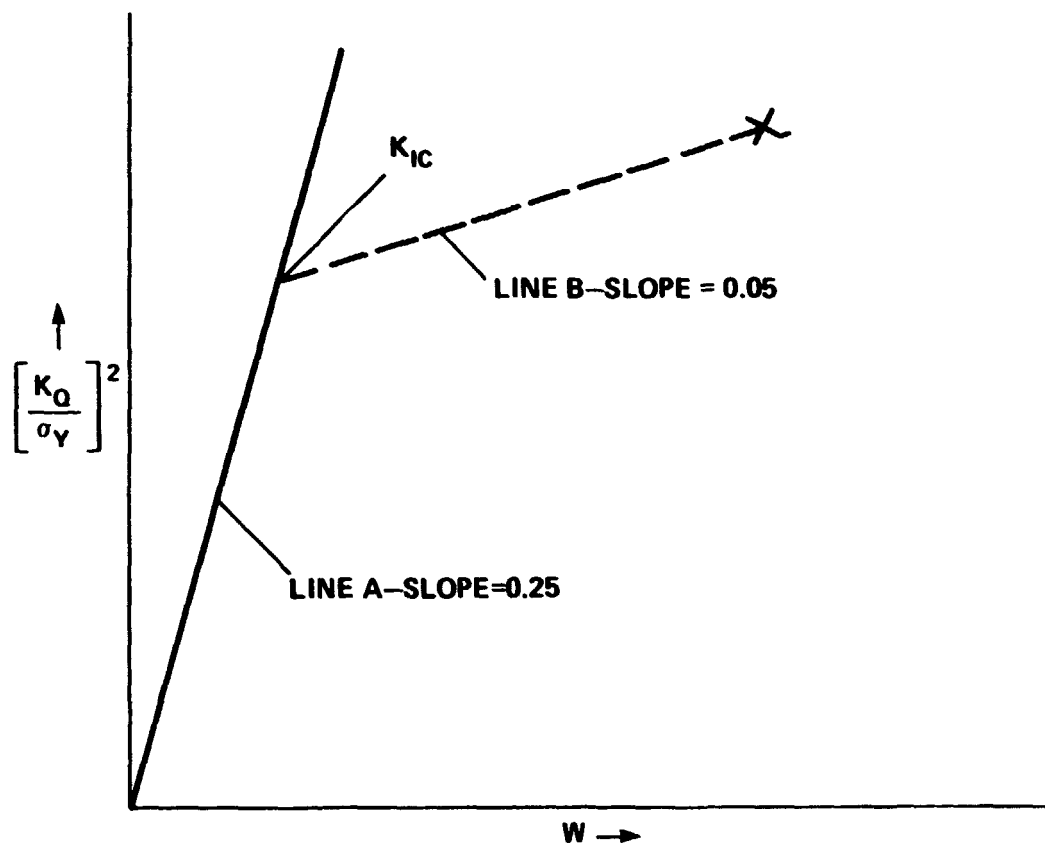


FIG. 12 - An outline of the proposed approach for the determination of  $K_{IC}$  in a CT specimen with  $a/W = 0.5$ .